

## Supporting Information

### **Towards Universal Luminescence Protein Post-Translational modification in High Throughput format**

Harri Härmä<sup>1\*</sup>, Natalia Tong-Ochoa<sup>1</sup>, Arjan J. van Adrichem<sup>2</sup>, Ilian Jelesarov<sup>3</sup>,  
Krister Wennerberg<sup>2</sup>, Kari Kopra<sup>1</sup>

1) Materials Chemistry and Chemical Analysis, University of Turku, Turku, Finland

2) Institute for Molecular Medicine Finland, FIMM, Helsinki, Finland

3) Department of Biochemistry, University of Zurich, Zurich, Switzerland

\*Corresponding author: harri.harma@utu.fi

## **Table of contents**

### **1. Materials and methods**

1.1 Materials

1.2 Instrumentation

1.3 Experimental procedures

1.3.1 CD spectroscopy of the leucine zipper peptides

1.3.2 Europium-chelate conjugation of the detection peptides

1.3.3 Homogeneous binding tests for the leucine zipper complex formation

1.3.4 Enzyme activity monitoring using the peptide-break technology

1.3.5 Data analysis

### **2. Results and discussion**

## 1. Materials and methods

### 1.1 Materials

All peptides were purchased from Pepmic Co., Ltd (Suzhou, China) and QRET Technologies (Turku, Finland). Used enzymes; catalytic domain of EGFR (part no. PR7295B), catalytic domain of PKA (part no. P6000L), recombinant human Sirt1 (part no. S35-31H), recombinant human HDAC3/NcoR2 (part no. H85-38G), recombinant human PTP1B (part no. 10010896), and recombinant human HDAC3/NcoR2 (part no. H85-38G) were from Thermo Fisher Scientific (Waltham, CA), New England Biolabs (Ipswich, MA), SignalChem (Richmont, Canada), BPS Bioscience (San Diego, CA), and Cayman Chemical (Ann Arbor, MI). TCS-401, SRT 1720, TSA, GSK484, and PD 174265, NAD<sup>+</sup> free acid cofactor, were from Cayman Chemical. Nonadentate europium-chelate-9d, {2,2',2'',2'''}-[2-(4-isothiocyantophenyl)ethylimino]-bis(methylene)bis{4-{4-(agalactopyranoxy)phenyl}ethynyl}-pyridine-6,2-diyl}bis(methylenenitrilo)} tetrakis(acetato)europium(III) was purchased from BN Products&Services (Turku, Finland). The soluble modulator molecule MT2 was from QRET Technologies. AG-1478, Compound 56, and erlotinib were from Cell Signaling Technology (Danvers, MA). H-7 dihydrochloride, H-89 dihydrochloride, and EX-527 were from Santa Cruz Biotechnology (Dallas, TX). Na<sub>3</sub>VO<sub>4</sub> was from MP Biomedicals (Santa Ana, CA). Eu<sup>3+</sup>-standard solution and black microtiter plates, Optiplate 384F were from PerkinElmer Life and Analytical Sciences, Wallac (Turku, Finland). All other reagents, including analytical-grade solvents, ATP, and staurosporine were acquired from Sigma-Aldrich (St. Louis, MO).

### 1.2 Instrumentation

Europium-peptide conjugates were purified using a reversed-phase liquid chromatography, Dionex ultimate 3000 LC system from Thermo Fischer Scientific, Dionex (Sunnyvale, CA, USA), and the Ascentis RP-amide C18 column from Sigma-Aldrich, Supelco Analytical (St. Louis, MO, USA). Time-resolved luminescence (TRL)-signal was measured with standard Labrox plate reader from Labrox Ltd, using 340 nm excitation and 615 nm emission wavelengths, 600 μs delay time, and 400 μs decay time. Circular dichroism (CD) was carried out with a Chirascan CD spectrometer from Applied Photophysics Ltd. (Leatherhead, UK). CD signal was monitored from 190 to 250 nm in 1 nm steps with an averaging time of 5 s at each wavelength.

### 1.3 Experimental procedures

#### 1.3.1 CD spectroscopy of the leucine zipper peptides

Non-labeled leucine zippers (Jun/pJun and Fos) and (Tyro-LZ/TyroP-LZ and non-labeled EuLZ) were diluted to PBS (pH 7.4) at a 30 μM concentration.

Wavelength scans were measured at RT in a 1 mm cuvette. Three replicates for each sample were monitored and the signal average was considered after signal subtraction of the buffer solution alone.

### 1.3.2 Europium-chelate conjugation

Fos and EuLZ detection peptides were labeled using Eu<sup>3+</sup>-chelate. The label (1 mg) was dissolved into 100 µl of water and mixed with 100 µl of peptide (0.5 mg) in pyridine/H<sub>2</sub>O/triethylamine solution as previously described<sup>1</sup>. The conjugation reaction was incubated at room temperature (RT) for 18 h and the labeled europium-peptide was purified with HPLC. After purification, Europium-peptide concentration was determined based on the Eu<sup>3+</sup>-ion concentration by comparing observed luminescence signal to a commercial Eu<sup>3+</sup>-standard<sup>2</sup>.

### 1.3.3 Homogeneous binding tests for the leucine zipper complex

Peptide binding tests were performed for the Fos-Jun leucine zipper and modified leucine zippers in a homogeneous assay format using the Assay buffer containing 10 mM HEPES (pH 7.5), 0.1 mM EDTA, 0.01% Triton, 5 mM NaCl, and 1 mM MgCl<sub>2</sub>. To understand the affinity of the peptide pairs, the phosphorylated (pJun and TyroP-LZ) and non-phosphorylated (Jun and Tyro-LZ) peptides were titrated at concentrations from 0.1 nM to 15 µM using 0.5 nM of EuLZ for Tyro-LZ/TyroP-LZ and 2 nM of Fos for Jun/p-Jun peptides as a labeled counterpart. Peptides were incubated in a 30 µl volume for 5 min in a 384-well plate and 20 µl of soluble quencher was added according to the manufacturer's instruction. TRL-signals were monitored at the 30 min time point.

### 1.3.4 Enzyme activity monitoring using the peptide-break technology

All enzymatic assays were carried out in a 384-microtiter plate well. A typical enzymatic assay was performed in a 10 µl volume and incubated in a plate shaker at RT for 30-45 min. Thereafter, the detection components were added in a 40 µl volume reaching the 50 µl final volume. The incubation was continued for 30 min prior to the TRL-signal measurements. Enzymatic reactions for kinases (PKA and EGFR) and phosphatase (PTP1B) were performed in the Assay buffer. For deacetylases (Sirt1 and HDAC3), the Assay buffer was supplemented with 25 mM NaCl and 2.7 mM KCl. Citrullination was carried out in a buffer containing 50 mM HEPES (pH 7.5), 25 mM NaCl, and 0.01% Triton X-100. In all assays, the detection components were added in the Assay buffer. The dose-response measurements of inhibitor and activator panels from 0 to 100 µM were performed to validate the enzymatic assays.

**Table S1.** Peptide-break assay conditions for the selected enzyme targets. Concentrations are given considering the final volume of 50  $\mu$ l per well.

Enzyme target	Enzymatic assay components			Detection components	
	Peptide substrate (nM)	Enzyme (nM)	Cofactor ( $\mu$ M)	EuLZ (nM)	MT2 ( $\mu$ M)
EGFR	10	0.5	50 (ATP)	10	3
PKA	10	0.5	50 (ATP)	10	3
PTP1B	10	3.0	-	10	3
Sirt1	20	0.5 / 0.05 <sup>1</sup>	500 (NAD <sup>+</sup> )	5	2
HDAC3	10	0.5	-	10	3
PAD4	10	1.0	-	10	3

<sup>1</sup>Low enzyme concentration was used to obtain improved assay window for the activator.

A kinetic assay format was demonstrated for EGFR and PKA to support continuous phosphorylation activity monitoring. Reactions were performed in a 20 $\mu$ l final volume. The PKA assay was carried out with 2 nM Ser-LZ substrate peptide, 1 nM PKA, 50  $\mu$ M ATP, 1 nM EuLZ, and 1.5  $\mu$ M soluble MT2. The EGFR assay was performed with 8 nM Tyro-LZ, 1 nM EGFR, 50  $\mu$ M ATP, 3 nM EuLZ, and 1.5  $\mu$ M soluble MT2. In the protocol, inhibitor, substrate peptide, EuLZ and MT2 were added to the well in 14  $\mu$ l and incubated with plate shaker at RT for 5 min. Thereafter premixed kinase and ATP solution was added to the well in a 6  $\mu$ l volume. The first TRL-signal was measured immediately after the enzyme and cofactor addition (“0 time point”).

The kinase assays were also miniaturized to a 10 $\mu$ l final volume. The effect of the DMSO in the assay performance was studied using PKA assay in the presence of varying concentration of DMSO (0-10%) in the Assay buffer. The reaction utilized 10 nM peptide substrate, 50  $\mu$ M ATP, and 0.5 nM PKA/1 nM EGFR. For the detection, 10/5 nM of EuLZ and 3/2  $\mu$ M soluble MT2 were applied for the PKA and EGFR assays, respectively. The miniaturized peptide-break technology was further validated by running a phosphorylation inhibitor screen for PKA and EGFR with 356 compounds from the PKIS library. The screens were performed in singlets with 1  $\mu$ M PKIS inhibitor concentration and 0 and 1  $\mu$ M staurosporine as controls calculated to 10  $\mu$ l and TRL-signals were monitored at 60 min time point. The assay robustness with calculated Z' factor was evaluated considering 96 data points for each 0 and 1  $\mu$ M staurosporine concentration from three assayed plates.

### 1.3.5 Data analysis

In all assays, the signal-to-background ratio (S/B) was calculated according to  $\mu_{\max}/\mu_{\min}$ , and the coefficient of variation (CV%) was  $(\sigma/\mu)*100$  where  $\mu$  is the mean value and  $\sigma$  the standard deviation. The threshold values for the PKIS PKA screen was calculated according to  $\mu_{\min} + 3*\sigma_{\min}*100/\mu_{\max}$  using  $3*\sigma_{\min}$ .

In the CD experiments, raw data was obtained in millidegrees and was converted to mean residue ellipticity (MRE) using the following formula:

$$MRE = \frac{\theta}{10 \times l \times r \times c}$$

Where  $\theta$  is the sample CD signal in millidegrees,  $l$  the cell path length in centimeters,  $r$  the number of amino acids in the peptide, and  $c$  the total peptide concentration in molar. Origin 8 software was used to present all data.

## 2. Results and discussion

With the homogeneous peptide binding assays for Jun/pJun with Eu-labeled Fos and for Tyro-LZ/TyroP-LZ with Eu-labeled EuLZ peptides we aimed to understand the binding properties of the studied peptides. Higher affinity was observed for the Tyro-LZ/TyroP-LZ with EuLZ peptide, compared to the Jun/pJun peptides with Fos. Typically, a low nanomolar concentration of Tyro-LZ/TyroP-LZ with EuLZ peptides was sufficient to obtain the optimal working window with sufficient discrimination to modified vs. non-modified peptides and S/B over 5. This also extends to other PTM peptides tested. We ran inhibitor and activator dose-response curves for the target enzymes and calculated the  $IC_{50}$  values (Table S2). Under the used assay conditions, the dose-response data for inhibitors and activator for the specific enzymes gave corresponding values reported in the literature.

**Table S2:** Calculated and literature  $IC_{50}$  values and obtained S/B values using the universal peptide-break technology.

<i>Target enzyme</i>	<i>Inhibitor</i>	<i>S/B ratio</i>	<i>Experimental <math>IC_{50}</math> (nM)</i>	<i><math>IC_{50}</math> literature value (nM)</i>	<i>Reference</i>
EGFR	PD 174265	10	$0.9 \pm 0.2$	0.5	3
EGFR	Compound 56	12	$1.6 \pm 0.5$	3.2	4
EGFR	AG-1478	7.8	$0.9 \pm 0.1$	0.8	4
EGFR	Erlotinib	9.1	$0.7 \pm 0.1$	1.0	5
EGFR	Staurosporine	15	$246 \pm 61$	283	6
PKA	Staurosporine	60	$72 \pm 4$	80	7
PKA	H-7	62	$40200 \pm 2200$	3000	8
PKA	H-89	97	$241 \pm 21$	135	9
PTP1B	$Na_3VO_4$	7.6	$18 \pm 2$	46	10
PTP1B	TCS-401	4.1	$12700 \pm 2400$	5000	11
Sirt 1	EX527	6.1	$147 \pm 17$	160	12
HDAC3/NcoR2	TSA	6.0	$97 \pm 3$	21	14

For the kinetic measurement, reagent concentrations were optimized as the protocol differed from the end-point dose-response procedure. First the peptide-peptide complex was preformed in the presence of inhibitor and quencher. The enzymatic reaction was initiated by addition of premixed ATP and 1 nM kinase and the phosphorylation reaction was monitored in real-time (Fig. S1). The enzymatic activity of the PKA and EGFR were according to the manufacturers 5000 and 250 nmol/min/mg, respectively. Our kinetic data further corroborates the higher phosphorylation activity of PKA compared to EGFR.

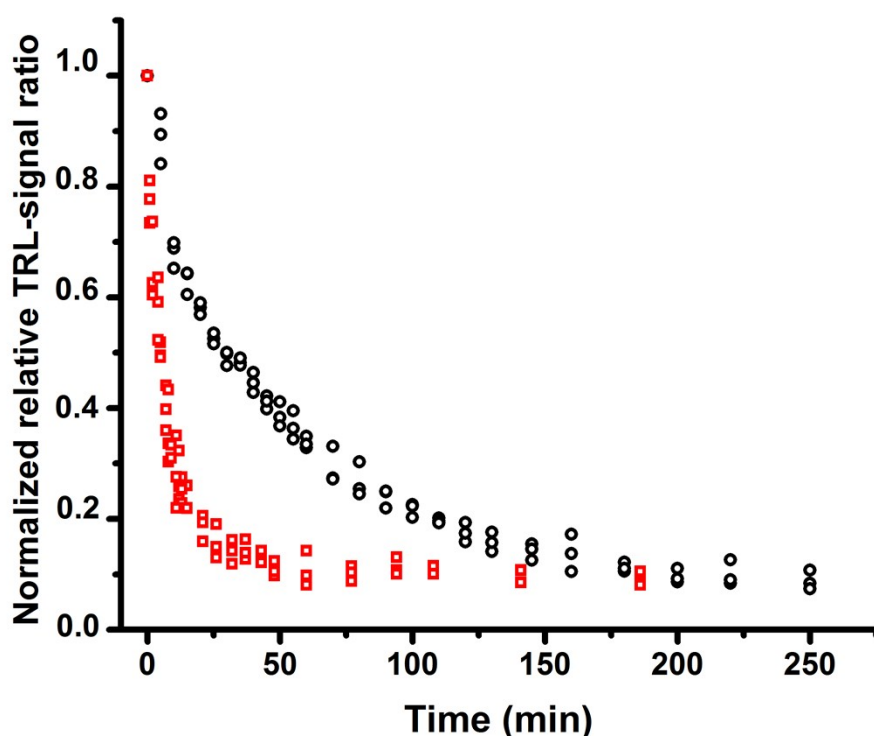


**Figure S1.** Kinetic measurement for EGFR (black) and PKA (red) kinase activity. The kinetic data was run at 1 nM enzyme concentrations in a 20  $\mu$ L volume.

Since DMSO is a common solvent used for preparing drug compound libraries, DMSO tolerance was evaluated in the miniaturized PKA assay performed in a 10  $\mu$ l final assay volume (Fig. S2). DMSO concentration up to 10% was well tolerated in the peptide-break assay with equal S/B ratio at all DMSO concentrations. Although the overall signals increased as the concentration of DMSO was increased, the S/B ratio remained unchanged.

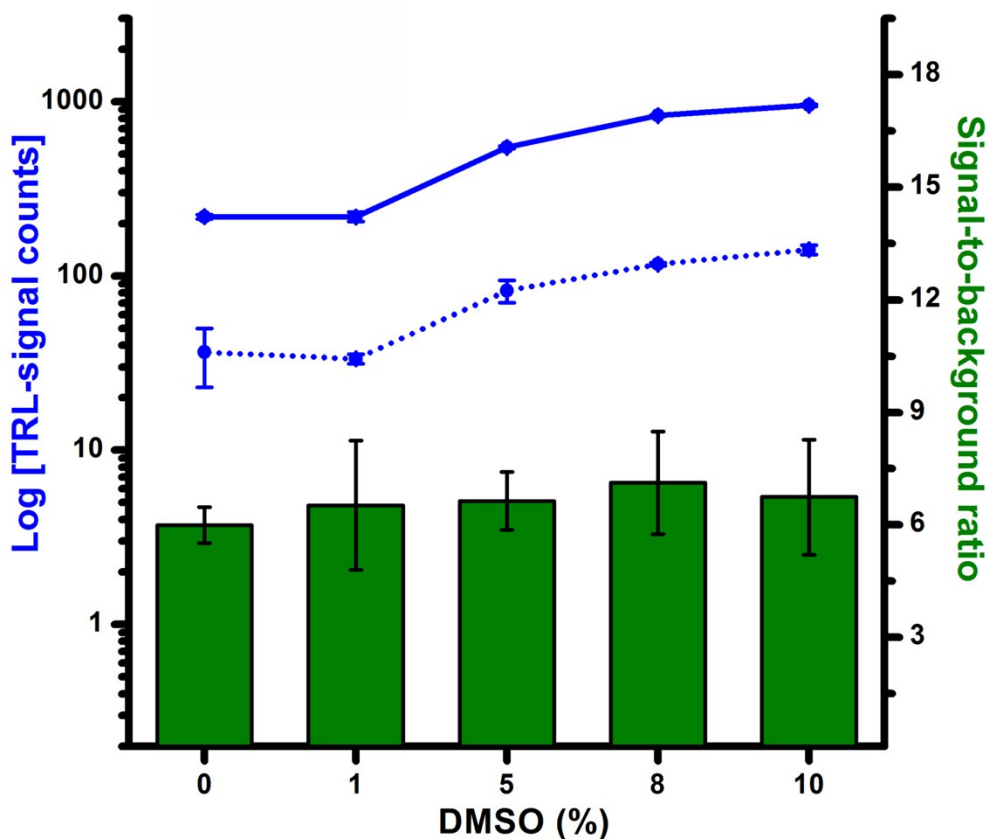


**Figure S2.** DMSO tolerance in the PKA kinase assay. Both phosphorylation and non-phosphorylation signals increase as the DMSO concentration increases.

The peptide-break technology was validated with a small-scale screen using the miniaturized assay format and selected 356-compound PKIS kinase library (Fig. S3). In the EGFR assay, 42 compounds were detected with the peptide-break system out of 48 compounds with activity  $< 1 \mu\text{M}$  according to the Nanosyn Caliper Screening data found from the ChEMBL online information<sup>15</sup>. For the hit identification we used a threshold of 6SD at compound concentration of  $1 \mu\text{M}$ .

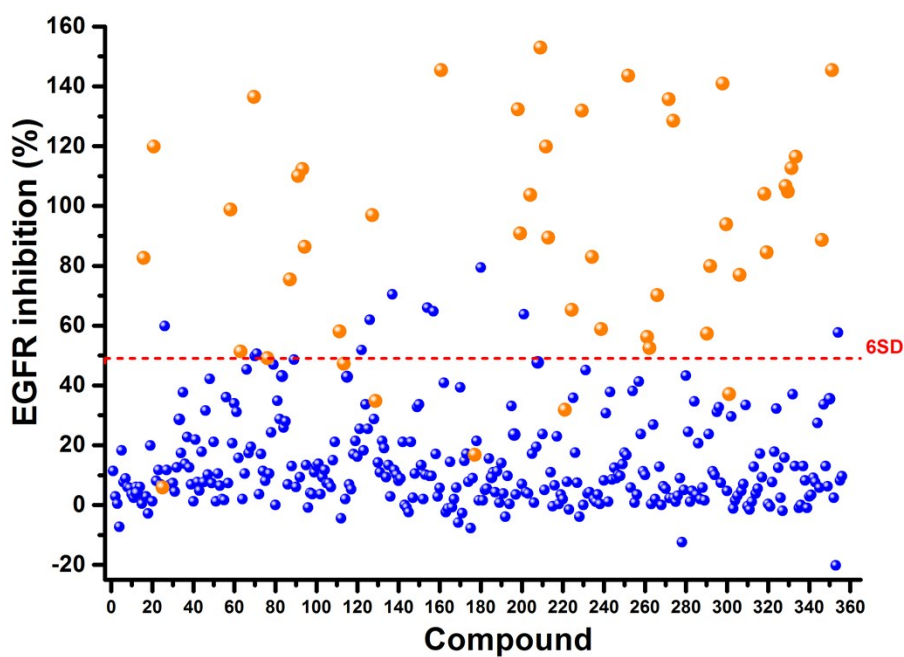


**Figure S3:** Validation of the universal peptide-break technology using selected PKIS compound library. PKIS screens for EGFR kinase was performed using 1 $\mu$ M inhibitor concentration and a 6SD threshold for hit identification was set for EGFR assay. Compounds with activity < 1  $\mu$ M detected with the Nanosyn Caliper screening are shown in orange<sup>15</sup>.

## References:

- (1) Tong-Ochoa, N.; Kopra, K.; Syrjänpää, M.; Legrand, N.; Härmä, H. *Anal. Chim. Acta* **2015**, *897*, 96.
- (2) Hemmilä, I.; Dakubu, S.; Mukkala, V.; Siitari, H.; Lövgren, T. *Anal. Biochem.* **1984**, *137*, 335.
- (3) Fry, D. W.; Bridges, A. J.; Denny, W.; Doherty, A.; Greis, K.; Hicks, J.; Hook, K.; Keller, P.; Leopold, W.; Loo, J.; McNamara, D.; Nelson, J.; Sherwood, V.; Smaill, J.; Trump-Kallmeyer, S.; Dobrusin, E. *Proc. Natl. Acad. Sci.* **1998**, *95*, 12022.
- (4) VanBrocklin, H. F.; Lim, J. K.; Coffing, S. L.; Hom, D. L.; Negash, K.; Ono, M. Y.; Gilmore, J. L.; Bryant, I.; Riese, D. J. *J. Med. Chem.* **2005**, *48*, 7445.
- (5) Suzuki, N.; Shiota, T.; Watanabe, F.; Haga, N.; Murashi, T.; Ohara, T.; Matsuo, K.; Oomori, N.; Yari, H.; Dohi, K.; Inoue, M.; Iguchi, M.; Sentou, J.; Wada, T. *Bioorganic Med. Chem. Lett.* **2011**, *21*, 1601.
- (6) Im, D.; Jung, K.; Yang, S.; Aman, W.; Hah, J. M. *Eur. J. Med. Chem.* **2015**, *102*, 600.
- (7) Pandey, A.; Volkots, D. L.; Seroogy, J. M.; Rose, J. W.; Yu, J. C.; Lambing, J. L.; Hutchaleelaha, A.; Hollenbach, S. J.; Abe, K.; Giese, N. A.; Scarborough, R. M. *J. Med. Chem.* **2002**, *45*, 3772.
- (8) Hidaka, H.; Inagaki, M.; Kawamoto, S.; Sasaki, Y. *Biochemistry* **1984**, *23*, 5036.
- (9) Davies, S. P.; Reddy, H.; Caivano, M.; Cohen, P. *Biochem. J* **2000**, *351*, 95.
- (10) Gordon, J. A. [41] *Use of vanadate as protein-phosphotyrosine phosphatase inhibitor*; 1991; Vol. 201.
- (11) Iversen, L. F.; Andersen, H. S.; Branner, S.; Mortensen, S. B.; Peters, G. H.; Norris, K.; Olsen, O. H.; Jeppesen, C. B.; Lundt, B. F.; Ripka, W.; Møller, K. B.; Møller, N. P. *J Biol Chem* **2000**, *275*, 10300.
- (12) Rotili, D.; Tarantino, D.; Carafa, V.; Paolini, C.; Schemies, J.; Jung, M.; Botta, G.; Di Maro, S.; Novellino, E.; Steinkühler, C.; De Maria, R.; Gallinari, P.; Altucci, L.; Mai, A. *J. Med. Chem.* **2012**, *55*, 8193.
- (13) Milne, J. C.; Lambert, P. D.; Schenk, S.; Carney, D. P.; Smith, J. J.; Gagne, D. J.; Jin, L.; Boss, O.; Perni, R. B.; Vu, C. B.; Bemis, J. E.; Xie, R.; Disch, J. S.; Ng, P. Y.; Nunes, J. J.; Lynch, A. V.; Yang, H.; Galonek, H.; Israelian, K.; Choy, W.; Iffland, A.; Lavu, S.; Medvedik, O.; Sinclair, D. A.; Olefsky, J. M.; Jirousek, M. R.; Elliott, P. J.; Westphal, C. H. *Nature* **2007**, *450*, 712.
- (14) Muthyala, R.; Shin, W. S.; Xie, J.; Sham, Y. Y. *Bioorganic Med. Chem. Lett.* **2015**, *25*, 4320.
- (15) Elkins, J. M.; Fedele, V.; Szklarz, M.; Abdul Azeez, K. R.; Salah, E.; Mikolajczyk, J.; Romanov, S.; Sepetov, N.; Huang, X. P.; Roth, B. L.; Al Haj Zen, A.; Fourches, D.; Muratov, E.; Tropsha, A.; Morris, J.; Teicher, B. A.; Kunkel, M.; Polley, E.; Lackey, K. E.; Atkinson, F. L.; Overington, J. P.; Bamborough, P.; Muller, S.; Price, D. J.; Willson, T. M.; Drewry, D. H.; Knapp, S.; Zuercher, W. J. *Nat. Biotechnol.* **2016**, *34*, 95.